THE JOURNAL OF BIOLOGICAL CHEMISTRY VOL. 290, NO. 3, pp. 1804–1817, January 16, 2015

A Novel Isoform of Met Receptor Tyrosine Kinase Blocks Hepatocyte Growth Factor/Met Signaling and Stimulates Skeletal Muscle Cell Differentiation*

Received for publication, July 24, 2014, and in revised form, December 2, 2014 Published, JBC Papers in Press, December 3, 2014, DOI 10.1074/jbc.M114.596957

Minseon Park[‡1], **Bok-Soon Lee**[§], **Soung-Hoo Jeon**[‡2], **Hyun-Ja Nam**[‡3], **Gwang Lee**[¶], **Chul-Ho Kim**[§], **Hyeseong Cho**[‡], **and Jae-Ho Lee**[‡4]

From the Departments of [‡]*Biochemistry and Molecular Biology,* [§]*Otolaryngology, and* [¶]*Physiology, Ajou University School of Medicine, Yeongtong-gu, Suwon 443-721, Korea*

Background: Alternative splicing gives a variation from the same gene.
Results: A novel alternative splicing form of Met exists in human skeletal muscle, and its depletion decreases muscle differentiation, whereas its overexpression acts oppositely.
Conclusion: A novel alternative splicing form of Met regulates skeletal muscle differentiation.
Significance: This is an example of regulation by alternative splicing, which affects skeletal muscle differentiation.

Hepatocyte growth factor (HGF) and its receptor, Met, regulate skeletal muscle differentiation. In the present study, we identified a novel alternatively spliced isoform of Met lacking exon 13 (designated Δ13Met), which is expressed mainly in human skeletal muscle. Alternative splicing yielded a truncated Met having extracellular domain only, suggesting an inhibitory role. Indeed, Δ13Met expression led to a decrease in HGF-induced tyrosine phosphorylation of Met and ERK phosphorylation, as well as cell proliferation and migration via sequestration of HGF. Interestingly, in human primary myoblasts undergoing differentiation, Δ13Met mRNA and protein levels were rapidly increased, concomitantly with a decrease in wild type Met mRNA and protein. Inhibition of Δ13Met with siRNA led to a decreased differentiation, whereas its overexpression potentiated differentiation of human primary myoblasts. Furthermore, in notexin-induced mouse injury model, exogenous Δ13Met expression enhanced regeneration of skeletal muscle, further confirming a stimulatory role of the isoform in muscle cell differentiation. In summary, we identified a novel alternatively spliced inhibitory isoform of Met that stimulates muscle cell differentiation, which confers a new means to control muscle differentiation and/or regeneration.

Myogenic differentiation is a cascade of intracellular events involving the coordination of muscle-specific gene expression and exit from the cell cycle, resulting in terminally differentiated myotubes. The ability of adult muscle tissue to grow or regenerate in response to injury depends on the activation and proliferation of quiescent satellite cells in response to growth stimuli (1, 2). Their progeny myoblasts proliferate and eventually fuse with each other to replace degenerated muscle fibers in the injured area (3). Several growth factors and cytokines are implicated in stimulating or inhibiting satellite cell proliferation and differentiation (4–6).

Activation of Met receptor tyrosine kinase upon binding with hepatocyte growth factor (HGF)[5] induces pleiotropic responses, such as proliferation, motility, morphogenesis, and angiogenesis in several cell types including tumor cells (7) and functions in vertebrate development (8–11). In muscle, HGF is responsible for the proliferation of quiescent satellite cells and is involved in muscle regeneration (12). Met is expressed on quiescent satellite cells in normal muscle tissue (13), and the addition of HGF to cultured satellite cells promotes the entry into the cell cycle (14–16). In addition, HGF/Met signaling is required for the migration of satellite cells to injured site (17). Although HGF can increase the number of myoblasts in regenerating muscle, it conversely inhibits muscle differentiation *in vivo* and *in vitro* (18, 19), which is one example of the widely accepted dogma that differentiation and proliferation are opposite processes. Thus, HGF/Met signaling needs to be tightly regulated during the muscle differentiation process; it should be turned on at the early phase to activate the satellite cells and increase the progeny myoblasts but turned off at the late phase to induce terminal differentiation. The regulation of HGF/Met signaling during the muscle cell differentiation/regeneration is known to be achieved mainly by regulating expression levels of HGF and/or Met during muscle regeneration (18, 20–22).

Alternative splicing is one of the regulated processes during gene expression that generates structural or functional diversities necessary to regulate various physiological processes including development and differentiation. Several spliced Met

* This work was supported by National Research Foundation of Korea Grant 2011-0030043 funded by the Korean government (Ministry of Science, ICT, and Future Planning).
[1] Present address: Dept. of Biochemistry and Molecular Biology, Miller School of Medicine, University of Miami, Miami, FL 33136.
[2] Present address: Dept. of Microbiology and Immunology, Seoul National University College of Medicine, Seoul 110-799, Korea.
[3] Present address: Dept. of Pediatric and Adolescent Medicine, Mayo Clinic College of Medicine, Rochester, MN 55905.
[4] To whom correspondence should be addressed: Dept. of Biochemistry and Molecular Biology, Ajou University School of Medicine, 5 Woncheon-dong, Yeongtong-gu, Suwon 443-721, Korea. Tel.: 82-31-219-5053; Fax: 82-31-219-5059; E-mail: jhlee64@ajou.ac.kr.

[5] The abbreviations used are: HGF, hepatocyte growth factor; TA, tibialis anterior; hrGFP, humanized *Renilla* green fluorescence protein; CM, conditioned medium.

variants have been reported, such as an 8-kb major Met transcript, a 7-kb Met transcript, and Sm-Met, a small isoform of Met (23). However, except for the 8-kb major Met transcript, which yields the wild type Met protein, no known splice isoforms of Met are shown to be involved in normal human physiology.

In the present study, we found a novel alternatively spliced form of Met lacking exon 13, which yielded a C-terminal truncated Met protein having dominant negative activity. The inhibitory Met variant was induced in primary human skeletal muscle myoblasts at the onset of differentiation, stimulating differentiation process both *in vitro* and *in vivo*. Although the role of Met variants in the skeletal muscle differentiation is poorly understood, this study provides evidence that HGF/Met signaling during the skeletal muscle differentiation is inhibited by increasing the expression level of inhibitory Met variant, as well as decreasing the level of wild type Met via alternative splicing.

EXPERIMENTAL PROCEDURES

Reagents and Antibodies—Phosphotyrosine 4G10, human Met DO-24, and human Met DL-21 antibodies were from Upstate Biotechnology (Lake Placid, NY). Anti-phospho-p44/p42 MAP kinase (pERK1/2) and anti-p44/p42 MAP kinase (ERK1/2) were from Cell Signaling Technology (Mississauga, Canada). C-28 antibody for human Met and B-2 antibody for murine Met were purchased from Santa Cruz Biotechnology, Inc. (Santa Cruz, CA), and HGF antibody was from R&D Systems (Minneapolis, MN). Cy3-conjugated goat anti-mouse IgG was obtained from Jackson ImmunoResearch Laboratories, Inc. (West Grove, PA). Recombinant human HGF was generously provided by Dr. G. F. Vande Woude (Van Andel Research Institute, Grand Rapids, MI). HGF concentrations are presented as scatter units/ml, and 5 units are equivalent to ~1 ng of protein. RPMI 1640 medium, DMEM, minimum essential medium, F-10 medium, FBS, horse serum, trypsin-EDTA, antibiotic-antimycotic containing penicillin G sodium, streptomycin sulfate, and amphotericin B were obtained from Invitrogen. Protease inhibitor mixture tablet was purchased from Roche Applied Science. Phosphatase inhibitors and other reagents not specified were from Sigma.

Cell Culture and Transfections—NIH3T3 cells were obtained from American Type Culture Collection (Manassas, VA) and cultured in DMEM supplemented with 10% FBS. Transfections were performed using the Lipofectamine Plus™ (Invitrogen) according to the manufacturer's directions. The plasmid encoding human Met was a gift from Dr. G. F. Vande Woude. To generate Δ13Met-overexpressed NIH3T3 cells, cells were co-transfected with a plasmid pSV2neo conferring resistance to G418 and a plasmid encoding the Δ*13met* gene. Control cells were transfected with the resistance plasmid and empty vector. Cells were selected for 2 weeks with 800 μg/ml G418 and then grown as pools.

Lentiviral Vector Production—The control lentiviral vector plasmid (pLenti-hrGFP) expresses humanized *Renilla* green fluorescent protein (hrGFP; Stratagene) driven by human $EF1_{\alpha}$ gene promoter (24). To increase the expression of reporter gene, hrGFP gene was linked to the Woodchuck hepatitis virus post-transcriptional regulatory element (WPRE) as previously described (25). Human $EF1_{\alpha}$ gene promoter and WPRE were kind gifts from Dr. Dong Wan Kim (Changwon National University, Korea) and Dr. Thomas J. Hope (Salk Institute, CA), respectively. To construct Δ13Met lentiviral vector plasmid (pLenti-Δ13Met), hrGFP plus WPRE fragment in the pLenti-hrGFP vector was replaced with human Δ*13met* gene. High titer lentiviral vector stock was produced in 293T cells by calcium phosphate-mediated transient transfection of the pseudotyped lentiviral vectors (hrGFP or Δ13Met) along with packaging vectors as described (26).

RT-PCR—Total RNA from cultured cells or tissue samples (3 μg) was used as template for first strand cDNA synthesis using AMV reverse transcriptase (TaKaRa Bio Inc.) according to the manufacturer's directions. PCR amplifications were subsequently performed using 5% of the first strand cDNA mixture and specific primers for human Met (NM_000245): primer 1, 5′-CTCATTTATGTACATAATC-3′; primer 2, 5′-AGGCCCAGATCTCTAT-3′; primer 3, 5′-GCTAAATATAGAGATCTGC-3′; primer 4, 5′-CTGGAAAAGTAGCTCGGTAGTC-3′; human HGF (m29145), 5′-CCATGAATTTGACCTCTATG-3′ and 5′-AACTCGGATGTTTGGGTCA-3′ (783 bp); and human myogenin (BC053899), 5′-TGGAGCTGTATGAGACATCCC-3′ and 5′-GTCCACGATGGAGGTGAGGG-3′ (597 bp). Amplification of control β-actin mRNA was performed using primers 5′-CAGGTCCAGACGAGGATGGCAT-3′ and 5′-CGACATGGAAATCTGCACC-3′ (300 bp). The PCR cycling conditions were cycles of denaturation at 95 °C for 30 s, annealing at 53 °C for 30 s, and extension at 72 °C for 30 s and slightly modified depending on the target gene to amplify.

Immunoprecipitation and Western Blotting—Cells were lysed in radioimmune precipitation assay buffer (50 mM Tris-HCl, pH 7.4, 1% Nonidet P-40, 0.1% SDS, 150 mM NaCl, 5 mM EDTA) containing freshly added protease inhibitor mixture solution and/or phosphatase inhibitors (1 mM sodium fluoride and 1 mM sodium orthovanadate). Cell lysates (1 mg) were incubated with 1 μg of anti-Met antibody (C-28 or DO-24) for 16 h at 4 °C with gentle rotation. Then 20 μl of 50% slurry of rProtein G-agarose (Invitrogen) was added into each lysate, incubated for an additional hour, and centrifuged at 5,000 rpm for 3 min to collect immune complexes. The immunoprecipitates were washed three times with the lysis buffer and analyzed by immunoblotting. The protein expression was detected with ECL detection kit after incubation with HRP-conjugated secondary antibodies (Amersham Biosciences).

Immunofluorescence—Cells grown on glass coverslips were fixed by immersion in 4% paraformaldehyde for 15 min and permeabilized for 5 min in Tris-buffered saline containing 0.075% Triton X-100 (TBS-T). Nonspecific binding was blocked with 5% bovine serum albumin (BSA). Coverslips were then incubated with the primary antibody at room temperature in a humidified atmosphere. After three washes with PBS, the coverslips were incubated with Cy3-conjugated goat anti-mouse IgG antibody diluted in PBS containing 5% BSA, washed repeatedly with PBS, and mounted with Vectashield® mounting medium containing DAPI to visualize the nuclei (Vector Laboratories). To detect Met or myosin heavy chain (MHC), we

used DL-21 or MF-20 (Developmental Studies Hybridoma Bank, University of Iowa), respectively, and anti-desmin antibody was used to detect the myoblast-positive cells. Expression and localization of Met were observed under a confocal microscope (Olympus Fluoview FV300), and MHC was observed under a fluorescence microscope (Axio Imager; Carl Zeiss) using constant contrast and brightness conditions.

Subcellular Fractionation—To obtain the cytoplasmic fraction, cell pellets were resuspended in cytoplasmic buffer (20 mM Tris, 250 mM sucrose, 10 mM EGTA, and 2 mM EDTA, pH 7.5), incubated for 3 h on ice after sonication, and then centrifuged at 100,000 × *g* for 1 h at 4 °C. The insoluble pellet was resuspended in Nonidet P-40 buffer (20 mM Tris, 1% Nonidet P-40, 1 mM EGTA, and 1 mM EDTA, pH 7.5), incubated for 15 min on ice, and then centrifuged at 50,000 × *g* for 1 h at 4 °C to obtain the membrane fraction. Each fraction was resolved on 8% SDS-PAGE and immunoblotted with DL-21 antibody to detect Met isoforms. PKC-α (Santa Cruz, CA) was used as a marker for cytosolic fraction.

HGF Binding Assay—Δ13Met- or control vector-transfected NIH3T3 cell pools were plated at 5×10^6 cells in a 100-mm culture dish and cultured overnight. After washing three times with PBS, the cells were grown in 5 ml of DMEM, 0.02% FBS for another 24 h. Each conditioned medium (CM) was harvested, clarified by centrifugation, and concentrated 10-fold by using Centriplus® centrifugal filter devices (Millipore Co., Bedford, MA). The concentrated conditioned media were incubated with 100 ng of rhHGF for 16 h at 4 °C with rotating and then immunoprecipitated with anti-Met antibody (DO-24) or anti-HGF antibody. Western blot analysis was followed.

Cell Proliferation—Cells were seeded in 96-well plates and cultured overnight. After 24 h of serum starvation, the cells were incubated for the indicated time periods in the presence of HGF (20 units/ml). Cell numbers were counted after trypsinization using hemocytometer.

Scratch Wound Motility Assay—HaCaT cells were seeded (7×10^5 cells/well) in 24-well plates in RPMI 1640 supplemented with 10% FBS and allowed to adhere overnight. The cells were then starved with 0.1% FBS for 24 h. The monolayered cells were then carefully scratched with a sterile 200-μl pipette tip and incubated with the prepared conditioned media from Δ13Met- or control vector-transfected NIH3T3 cells for 48 h. After washing three times with cold PBS, the cells were fixed in acetone:methanol (1:1, v/v) for 15 min on ice and stained with 2% crystal violet. Cell migration was assessed by measuring the gap at three different sites and calculating the mean value.

Source of Human Skeletal Muscle—Skeletal muscle tissues were obtained from patients during surgical treatment for non-muscle problems of larynx. This study was approved by the Institutional Review Board of Ajou University Hospital (AJIRB-CRO-05-087), and all patients gave written informed consent.

Primary Skeletal Muscle Cell Culture—Primary skeletal muscle cells were isolated from the tissues according to a modified method of Foulstone *et al.* (27). Briefly, biopsy samples were dissected into 1-mm^3 pieces and digested in TE buffer (0.05% trypsin and 0.02% EDTA in PBS) for 1 h with gentle mixing at 37 °C. Then the reaction was stopped by adding FBS up to 10%, followed by filtration through 100-μm cell strainer (Falcon®; BD Biosciences) before centrifugation at 1000 rpm for 5 min. The cell suspensions were plated onto a 100-mm culture plate precoated with 0.2% gelatin, incubated, and passaged when 80–90% confluent. Cells in 80% confluence were induced differentiation by washing twice in PBS and adding the differentiation media (minimum essential medium supplemented with 2% horse serum, 50 IU/ml penicillin, and 50 μg/ml streptomycin). Isolated myoblasts were identified by immunostaining with anti-desmin antibody (Dako, Ely, UK). On average, primary cultures contained over 60% myoblasts, which did not change with passaging. All experiments were performed with cells between passages 2 and 5.

In Vivo Skeletal Muscle Regeneration—All experiments involving animals were guided by the Ajou University School of Medicine Institutional Animal Care and Use Committee. In C57BL/6 mice, tibialis anterior (TA) muscle was injured by the myotoxic agent notexin, as described previously (28). Briefly, mice were anesthetized with avertin (2,2,2-tribromoethanol; Sigma-Aldrich), and an adequate depth of anesthesia was maintained during the treatment. The right hind limb was shaved, and a small portion of the anterior aspect of the TA muscle was surgically exposed. Twenty μl of notexin (10 μg/ml in isotonic saline; Latoxan, Valence, France) was injected to the muscle with a 29-guage fixed needle, whereas the left leg was used as uninjected control. After intramuscular injection, the skin incision was closed with surgical sutures, and the mouse was allowed to recover in a warm place. Three days after notexin injection, the mouse was anesthetized, and the notexin-injected TA muscle was surgically exposed, and 300 ng of p24 of lentiviral stock was injected into the muscle. A group of mice was sacrificed on days 3, 6, 8, or 10 postinfection.

RNA Interference—Half million primary skeletal muscle cells were seeded in 60-mm culture dishes in antibiotic-free growing medium. After 24 h, cells were transfected with 100 nM siRNA per dish using Lipofectamine 2000 (Invitrogen). After 24 h, cells were washed twice with PBS, followed by shifting into differentiation medium. The siRNA target sequences for Δ13Met were 5′-AUAUAGAGAUCUGGGCAGUTT-3′. To deplete the human Met, three different siRNA sequences were used; 5′-GACCTTCAGAAGGTTGCTG-3′, 5′-GCCAGATTCTGCCGAACCA-3′, and 5′-GTGCAGTATCCTCTGACAG-3′ (29).

Immunohistochemical Analyses—At the time points indicated, TA muscles were harvested and fixed in 4% paraformaldehyde overnight, dehydrated, and embedded in paraffin. Sections for histological analysis (4–6 μm thick) were rehydrated and performed hematoxylin/eosin staining. The damaged area of transverse sections and cross-sectional areas of myofibers were measured using ImageJ version3.0 software and Carl Zeiss AxioVision version 4, respectively. The data are presented as the means ± S.D. The *p* values were determined using two-way analysis of variance or two-tailed unpaired Student's *t* test with statistical significance as indicated.

Statistical Analysis—The data are presented as the means ± S.D. The *p* values were determined using two-tailed unpaired Student's *t* test with statistical significance defined as $p < 0.05$.

RESULTS

A Novel Alternatively Spliced Form of Met Exists in Human Tissues—The Met receptor tyrosine kinase in mouse tissues is present as two major isoforms, and the only difference between these two forms is the presence of a 47-amino acid segment in the juxtamembrane region that can be deleted by alternative splicing of exon 14 (30). Because this segment is responsible for down-regulating activated Met, the smaller sized Met isoform lacking this segment is highly active (31).

To evaluate the presence of this isoform, which is called Sm-Met in human tissues, we amplified the cDNA region from exon 11 through exon 16 from the BD^{TM} human multiple tissue cDNA panel (Clontech) by using a specific primer set (Fig. 1A, *top panel*). In all tissues tested, an 806-bp band amplified from wild type c-*met* was observed, even though the expression levels were different among tissues under the same PCR conditions. Interestingly, an additional band was detected in the skeletal muscle sample below the 806-bp major band (Fig. 1*A*, *middle panel*). A similar band was observed in kidney, liver, pancreas, and placental tissues; however, the expression levels were much lower than that of skeletal muscle. To confirm the presence of the smaller band in tissues other than skeletal muscle, we amplified the same region from the liver cDNA by increasing the number of PCR cycles. As shown in Fig. 1*A* (*bottom panel*), two discrete bands were amplified after the PCR (first), and the reamplified bands from each band (second) clearly showed the presence of two different-sized cDNA fragments in liver tissue. To our surprise, sequencing analysis revealed that the smaller fragments from liver and skeletal muscle were not from exon 14 deletion. Instead, both liver and skeletal muscle lacked the 157-bp exon 13. The presence of this isoform was also confirmed in two different human primary skeletal muscle tissues by RT-PCR with other pairs of primers followed by sequencing (Fig. 1*B*).

Because the entire single transmembrane domain of Met is encoded by the second half of exon 13 (32), deletion of exon 13 in skeletal muscle or liver tissues is expected to eliminate the transmembrane domain of Met (Fig. 1*C*, *top panel*). Notably, exclusion of 157 bp should induce a frameshift, resulting in encoding five new amino acids followed by early termination (Fig. 1*C*, *middle panel*). Thus, the deduced protein of this variant is expected to contain only the extracellular domain and five additional amino acids (Ile-Trp-Ala-Val-Asp; Fig. 1*C*, *bottom panel*).

The Novel Isoform, Δ13Met, Yields a Detectable Protein in Vivo—Because not all alternatively spliced variants of Met yield detectable protein products *in vivo* (32, 33), we examined the expression of the encoded protein (hereafter designated as Δ13Met) in human primary skeletal muscle tissue, where the mRNA was abundantly found (Fig. 1*A*, *middle panel*). Lysates of primary skeletal muscle tissue and human Δ13Met-overexpressing NIH3T3 (Δ13Met-NIH3T3) cells were immunoprecipitated with the DO-24 anti-human Met antibody, and the precipitates were subjected to Western blotting with the DL-21 anti-human Met antibody (neither antibodies detect mouse Met). Because both antibodies target the extracellular portion of human Met, both wild type and Δ13Met could be detected. As shown in Fig. 1*D* (*top panel*), β-chains of Δ13Met (~100 kDa) and wild type Met (~145 kDa) were recognized in primary human skeletal muscle tissue. To determine the specificity of the detection, the blot was deprobed and then incubated with DL-21 anti-Met antibody, which had previously been adsorbed with Met antigenic peptide. As shown in Fig. 1*D* (*middle panel*), the Met and Δ13Met bands could no longer be detected, confirming the specificity. Next, the blot was reincubated with C-28 antibody raised against the C terminus of human Met (Fig. 1*D*, *bottom panel*). Although the band representing wild type Met was recovered, the presumed Δ13Met bands did not reappear because of a lack of the Met C terminus. Thus, these results suggest that a considerable amount of Δ13Met protein is expressed in human primary skeletal muscle tissue. The presence of Δ13Met protein was also evident from subsequent analysis using primary human myoblasts (see Fig. 4*D*).

Membrane-localized Δ13Met Is Shed into Culture Medium and Binds to HGF—To evaluate the localization of Δ13Met in cells, NIH3T3 cells were transfected with human Δ13Met or Met cDNA followed by immunostaining for human Met with DL-21 anti-Met antibody. Immunoreactivity of Met in Δ13Met-transfected NIH3T3 was detected in both cytoplasm and plasma membrane as in Met-transfected cells, which suggests that Δ13Met is localized in plasma membrane even though it lacks transmembrane and cytoplasmic domains (Fig. 2*A*). To confirm the presence of Δ13Met in plasma membrane, NIH3T3 cells were co-transfected with Δ13Met and Met cDNA followed by fractionation cytoplasm and membrane parts. Although a relatively larger amount of Δ13Met was observed in the cytoplasmic fraction, a small proportion was localized in the membrane fraction (Fig. 2*B*). It should be noted that the sizes of Δ13Met in the two fractions were different. It is highly likely that Δ13Met in the membrane represents a β-chain of the mature form, which is linked with α-chain in disulfide bond, whereas the cytoplasm contains only the premature form in which α- and β-chains are not yet cleaved by proteases. Our data therefore suggest that exogenously expressed Δ13Met is mainly present as an intracellularly localized precursor form, whereas a small amount is targeted to the plasma membrane as mature protein.

In view of the absence of the transmembrane domain, we examined whether Δ13Met is released into the culture medium after targeting to the membrane. Thus, the CM of Met- or Δ13Met-NIH3T3 cells was harvested, concentrated, and then subjected to Western blotting (Fig. 2*C*). Unexpectedly, a band of ~80 kDa that was smaller than Δ13Met was detected in the CM from both Met- and Δ13Met-NIH3T3 cells. This fragment represents a soluble, truncated form of Met that is released from the membrane-localized Met by proteolytic cleavage, *i.e.* ectodomain shedding, which is mediated by certain metalloproteases and occurs at or near the cell surface (34). Collectively, it is highly probable that Δ13Met is not secreted as itself but somehow localizes at the cell surface like peripheral protein and is shed into the medium.

Because the shedding Met released from the Met has binding ability with HGF because of the presence of the SEMA domain necessary for HGF binding (35), we examined whether the shedding Met cleaved from Δ13Met can also interact with

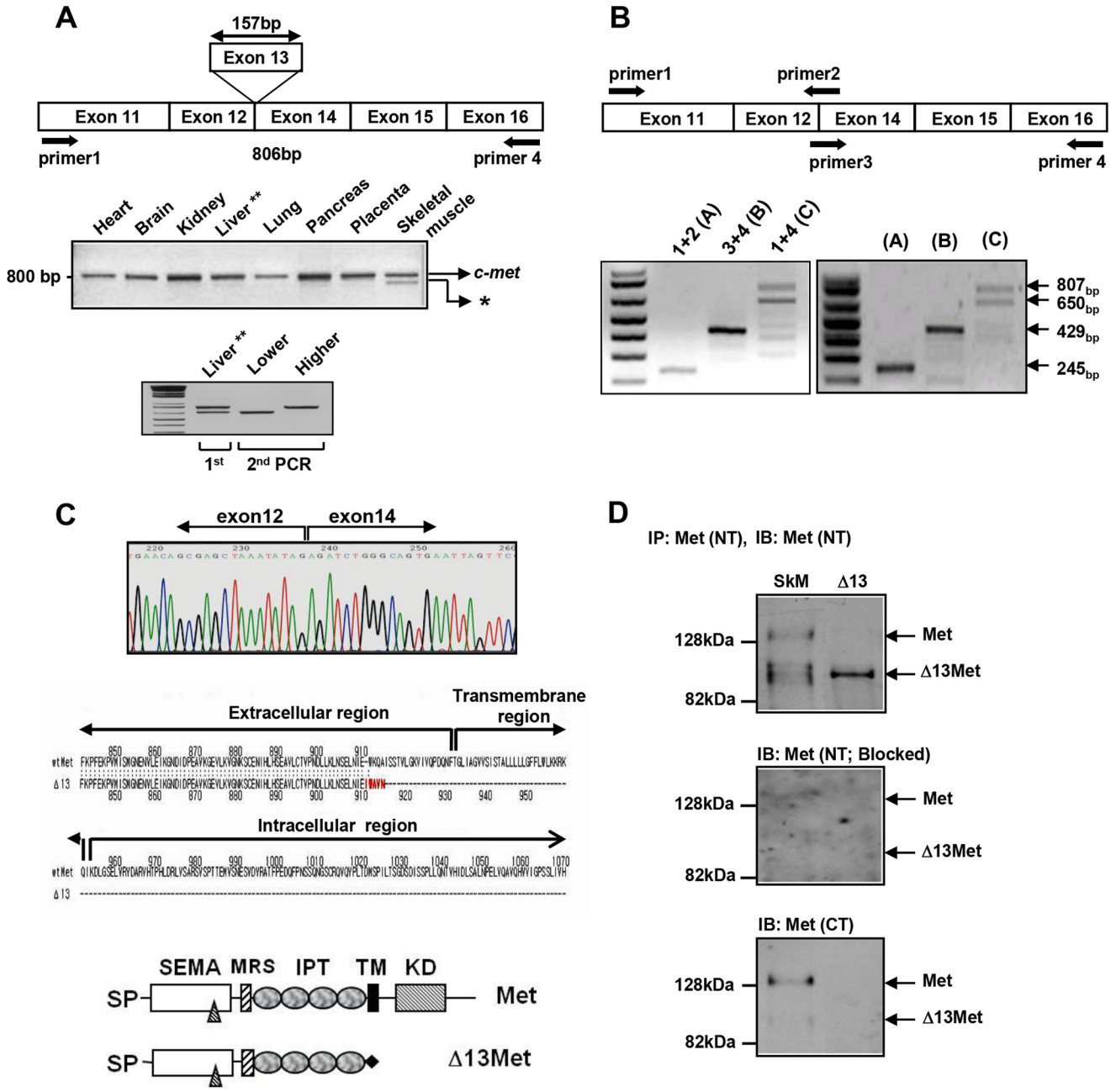

FIGURE 1. **A novel alternatively spliced form of *met* mainly expressed in human skeletal muscle tissue.** *A*, identification of a novel alternatively spliced form of Met. Amplification of c-*met* transcripts was performed using the Human Multiple Tissue cDNA Panel (Clontech) with PCR primers (*top panel*). *Middle panel*, *, a PCR product smaller than wild type c-*met*. *Bottom panel*, amplified bands (first PCR) from liver tissue (**) were eluted from the gel and reamplified with the same primers separately. *B*, RT-PCR was performed with different primer combinations (*top panel*). cDNA was reverse transcribed from the mRNAs of two different human skeletal muscle tissues followed by PCRs. *C*, DNA sequence analysis of the smaller PCR product was performed (*top panel*). Comparison of the deduced amino acid sequences between Met and Δ13Met (*middle panel*). Schematic representation deduced from the sequences of Δ13Met. *SP*, signal peptide; *SEMA*, semaphorin domain; *MRS*, Met-related sequence; *IPT*, immunoglobulin-plexin-transcription factor domain; *TM*, transmembrane domain; *KD*, kinase domain. The *triangles* signify proteolytic sites to generate α- and β-chains. The *diamond* represents newly translated five additional amino acids, resulting from exon 13 deletion-induced frameshift (*bottom panel*). *D*, detection of Δ13Met protein in human skeletal muscle tissue. *Top panel*, Met was immunoprecipitated (*IP*) from primary skeletal muscle tissue (*SkM*) with DO-24 and immunoblotted (*IB*) with DL-21; both antibodies recognize the different epitopes of N terminus of human Met (*NT*). NIH3T3 cells transfected with Δ13Met (*Δ13*) were used as the positive control. *Middle panel*, the *top blot* was deprobed and reincubated with DL-21 preabsorbed with Met antigenic peptide. *Bottom panel*, the *middle blot* was deprobed again and reincubated with C-28 antisera recognizing the C terminus of human Met (*CT*).

HGF. The results of IP-Western blotting of the conditioned media preincubated with rhHGF revealed that HGF co-immunoprecipitated with the shedding Met, which originated from Δ13Met and vice versa (Fig. 2*D*).

Δ13Met Attenuates HGF/Met Signaling—Upon binding with HGF, Met is dimerized and autophosphorylated on specific tyrosine residues, followed by transferring downstream signals including Ras-Raf-ERK (36). However, the presence of Δ13Met, which has no cytosolic domains, probably interferes with this HGF/Met signaling pathway by sequestering HGF.

To address this possibility, Δ13Met was transfected in NIH3T3 or human Met-overexpressed NIH3T3 cells followed

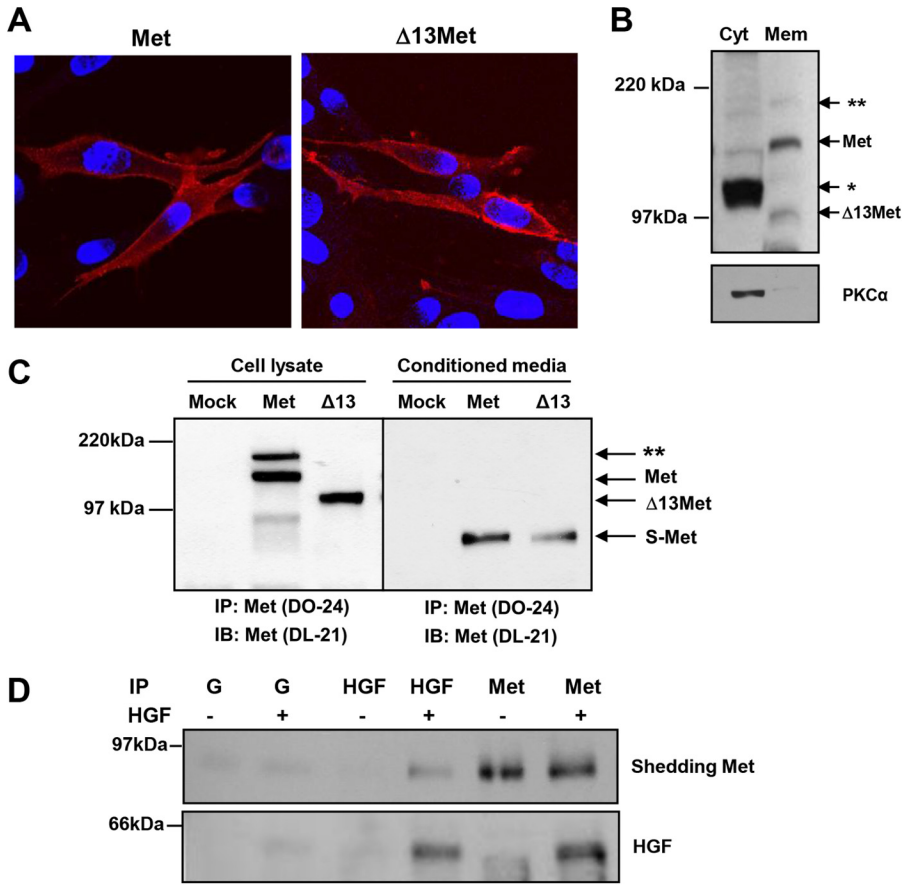

FIGURE 2. **Production of shedding Met with HGF binding ability from the membrane-localized Δ13Met.** *A*, intracellular localization of Met and Δ13Met. NIH3T3 cells seeded onto glass coverslips were transiently transfected with Met or Δ13Met. After 48 h, each protein was immunocytochemically visualized using DL-21 antibody. Nuclei were stained with DAPI. *B*, comparison of intracellular localization between Met and Δ13Met. NIH3T3 cells co-transfected with Met and Δ13Met were fractionated according to Nonidet P-40 solubility, followed by Western blotting using DL-21 antibody. *PKCα*, a marker of the cytosolic (*Cyt*) fraction. *, Δ13Met precursor; **, Met precursor. *C*, production of shedding Met from Δ13Met. NIH3T3 cells were transfected with Met, Δ13Met, or empty vector. Lysates or conditioned media from stable clones of each cDNA transfectant were immunoprecipitated (*IP*) with DO-24, and immunoblotted (*IB*) with DL-21. **, Met precursor; *S-Met*, shedding Met. *D*, HGF binding activity of shedding Met. Conditioned medium from Δ13Met-transfected NIH3T3 was incubated with or without 100 ng of HGF and immunoprecipitated with anti-HGF or DO-24 antibody, followed by Western blotting using DL-21 and anti-HGF antibodies. *Lanes G*, protein G, the negative control for immunoprecipitation.

by analyzing Met phosphorylation and ERK1/2 activation upon HGF stimulation by Western blotting. Δ13Met overexpression clearly decreased tyrosine phosphorylation of Met in the presence of HGF, as well as in the absence of HGF in both cell lines (Fig. 3*A*). Δ13Met also inhibited ERK1/2 phosphorylation by HGF in both cell lines, demonstrating that Δ13Met effectively inhibits HGF-induced downstream signaling. To further evaluate whether the inhibitory effect of Δ13Met on HGF/Met signaling pathway is dose-dependent, NIH3T3 cells were transfected with different concentrations of Δ13Met cDNA followed by stimulation with HGF. As shown in Fig. 3*B*, different amounts of Δ13Met led to a decrease in HGF-induced ERK1/2 phosphorylation in a concentration-dependent manner.

Because cell proliferation and migration are dependent on ERK1/2 signaling (37, 38), we also determined the inhibitory effect of Δ13Met on HGF-induced NIH3T3 cell proliferation. Overexpression of Δ13Met decreased cell proliferation compared with mock transfected NIH3T3 cells (Fig. 3*C*). In addition, the CM from Δ13Met-NIH3T3 cells prevented HGF-induced migration of HaCaT keratinocytes, whereas the CM from mock NIH3T3 cells did not affect cell migration (Fig. 3*D*), confirming the possible function of Δ13Met in sequestering HGF as a soluble Δ13Met. These findings collectively suggest that Δ13Met is capable of blocking HGF-induced cell proliferation and migration via inhibition of HGF/Met signaling in a concentration-dependent manner.

Δ13Met Is Induced during Skeletal Muscle Differentiation—Because a comparable level of Δ13Met was detected in skeletal muscle, it is possible that Δ13Met plays a physiological role in this tissue. Initially, we analyzed *de novo* HGF-dependent Met activation in primary human myoblasts cultured in growth medium (F-10 containing 20% FBS). Different batches of primary myoblasts were grown with or without neutralizing anti-HGF antibody for 48 h followed by immunoprecipitation with anti-Met antibody. As shown in Fig. 4*A*, although the extents were different between preparations, Met autophosphorylation was abolished by incubating with neutralizing antibody, suggesting that Met is activated by endogenous HGF.

Next, we evaluated the expression levels of Met and HGF during the differentiation of cultured myoblasts. Differentiated myoblasts displayed a characteristic multinucleated morphology and MHC induction in a time-dependent manner during the differentiation processes (Fig. 4*B*). As expected, the expression levels of c-*met* and *hgf* mRNA were maximal in actively

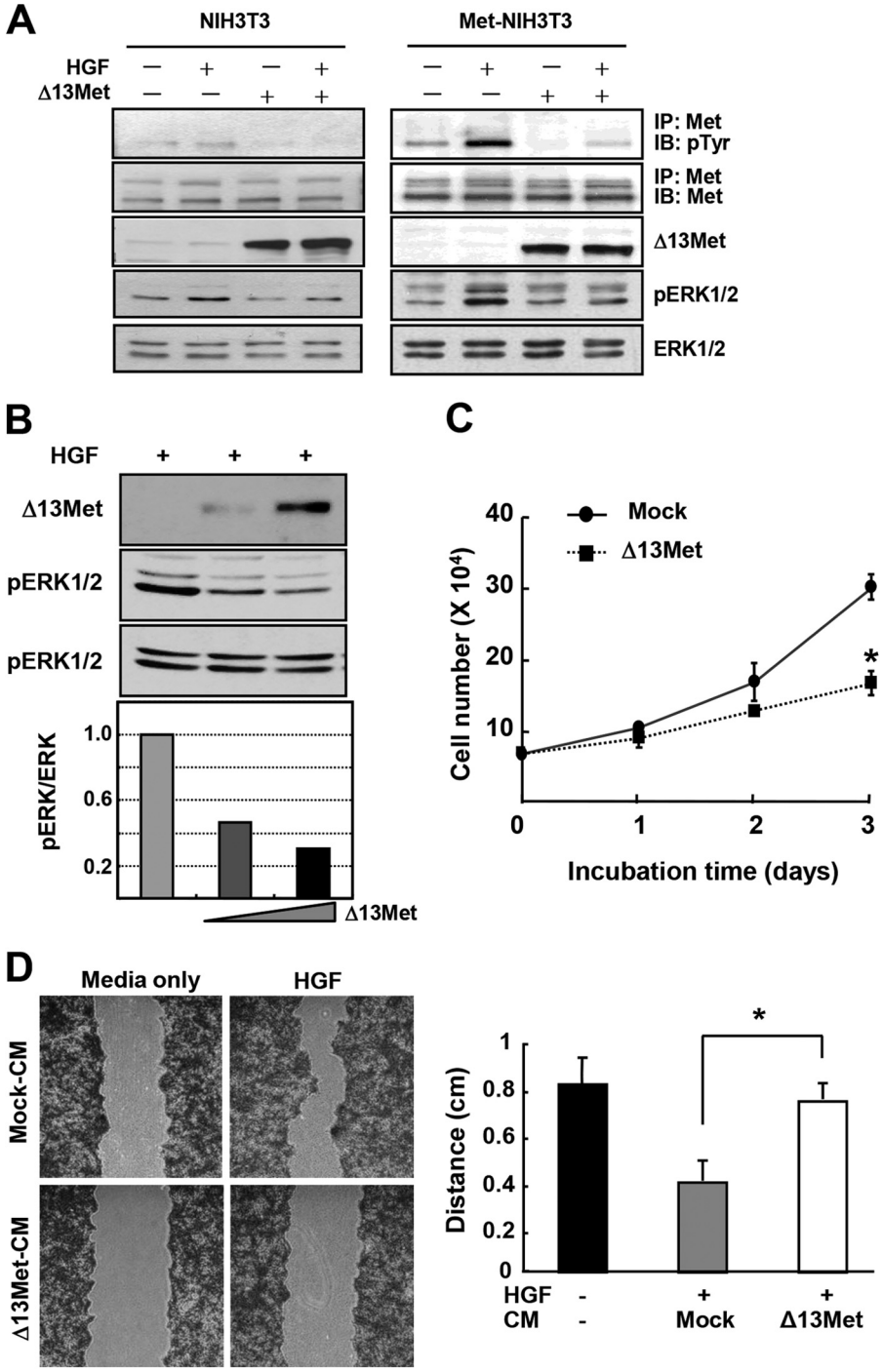

FIGURE 3. **Inhibition of HGF/Met signaling by Δ13Met.** *A*, effects of Δ13Met on Met activation and ERK phosphorylation. Δ13Met was transfected into NIH3T3 or Met-overexpressed NIH3T3 cells. After serum depletion for 24 h, cells were treated with 20 units/ml of HGF for 10 min. Lysates from the indicated samples were either analyzed directly by Western blotting for ERK phosphorylation (pERK1/2) or immunoprecipitated (*IP*) using B-2 (for murine Met, *left panel*) or DO-24 (for human Met, *right panel*) antibody, followed by Western blotting using the phosphotyrosine antibody (*pTyr*). Note that NIH3T3 cells express endogenous Met (31, 44, 45) as seen in the *left panel*. *IB*, immunoblotting. *B*, dose-dependent inhibition of HGF/Met signaling by Δ13Met. The lysates of NIH3T3 cells transfected with different doses of Δ13Met (0.5 or 3 μg per 60-mm dish) were subjected to Western blotting for ERK phosphorylation (*upper panel*). The ratio of pERK1/2 to ERK1/2 measured by densitometry (*bottom panel*). *C*, attenuation of cell proliferation by Δ13Met. The same number (1×10^4) of mock or Δ13Met-transfected NIH3T3 cells was seeded onto 96-well plates, followed by treatment with 20 units/ml HGF every 24 h. Cell growth was measured by cell counting. The data are presented as means ± S.D. of three independent experimental settings. *, $p < 0.05$. *D*, effect of shedding Met from Δ13Met on HaCaT cell migration. The wound healing ability of HaCaT cells was measured from the distance of the scratched area 48 h after incubation with conditioned medium from Δ13Met or mock transfected NIH3T3 cells in the presence of HGF (20 units/ml) in triplicate. Representative figures are shown (*left panel*). The data are presented as means ± S.D. *, $p < 0.05$.

proliferating myoblasts at day 0, followed by an evident decrease in the c-*met* transcript thereafter, but not *hgf* mRNA (Fig. 4*C*). On the other hand, the Δ*13met* transcript was barely detectable at day 0, but rapidly increased after the induction of differentiation as evidenced by myogenin expression, another marker for muscle differentiation. Consistent with RT-PCR

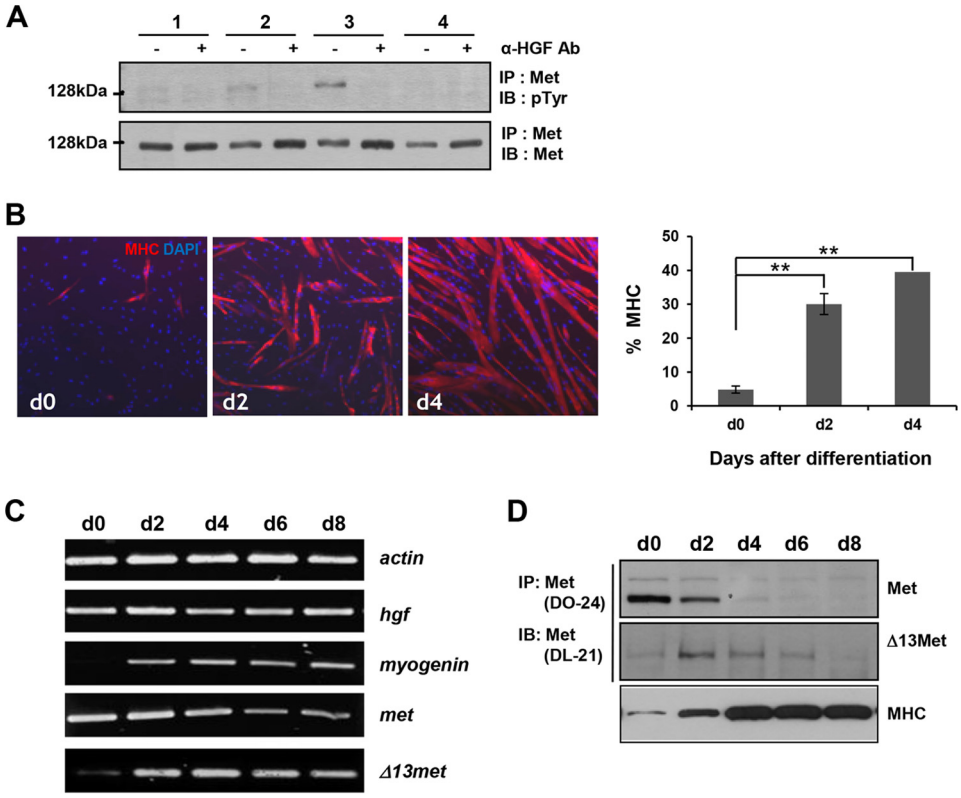

FIGURE 4. **Changes in Met and Δ13Met expression during differentiation of human primary skeletal muscle myoblasts.** *A*, HGF/Met signaling in human primary myoblasts. Primary cells were incubated with neutralizing anti-HGF antibody for 48 h in growth medium. Met phosphorylation was detected by immunoprecipitation (*IP*) with C-28 antibody, followed by Western blotting with phosphotyrosine antibody. The *numbers* denote different primary cell preparations. *B*, immunocytochemical analysis showing the expression of myosin heavy chain (*MHC*) in differentiated myoblasts. Primary myoblasts grown on coverslips were subjected to differentiation by switching to differentiation medium. After the indicated days, the cells were subjected to immunocytochemical analysis for MHC expression. Representative images are shown (*left panel*). Differentiation is represented by the percentage of MHC-positive cells of the total cells (*right panel*). Samples were analyzed in triplicate. The data are presented as means ± S.D. **, $p < 0.01$ compared with day 0. *C*, gene expression changes during differentiation. Primary myoblasts were induced to differentiate, and cells were harvested every 2 days. RT-PCR analysis was performed. Actin was used as the loading control. *D*, protein expression changes during myoblast differentiation. Primary cells were harvested every 2 days after differentiation. Cell lysates were immunoprecipitated with DO-24 and immunoblotted with DL-21 to detect Met and Δ13Met. *IB*, immunoblotting; *MHC*, a positive marker of differentiation; *d*, day.

data, Δ13Met protein expression was clearly increased 2 days after the induction of differentiation and gradually decreased thereafter, whereas Met expression gradually decreased during the whole period (Fig. 4*D*). These data indicate that although Δ13Met is an alternatively spliced form of Met, its expression is differently regulated from the Met expression during myoblast differentiation.

Suppression of Δ13Met Decreases Skeletal Muscle Differentiation—Because Δ13Met inhibits HGF/Met signaling and the expression of Met and Δ13Met are differently regulated during myogenic differentiation, it is highly probable that the concomitant increase of Δ13Met and decrease of Met expression are important for attenuating HGF/Met signaling, which is required for the transition to differentiation from proliferation of myoblasts.

To address this hypothesis, primary myoblasts were transfected with Δ13Met-specific siRNA followed by inducing differentiation. Δ13Met-specific siRNA was designed to target junctional sequences between exon 12 and exon 14 because the junction is the only region in *Δ13met* different from the wild type c-*met*. Therefore, use of another siRNA(s) of independent sequences was not an option. Specificity of the siRNA was demonstrated by Western blotting that only the protein level of Δ13Met but not Met was depleted by the siRNA in Met/Δ13Met-overexpressed NIH3T3 cells (Fig. 5*A*). When the primary myoblasts were induced for differentiation, Δ13Met siRNA-transfected primary myoblasts expressed myogenin mRNA 1 day later than control myoblasts, and the mRNA level slightly decreased on days 3 and 4 compared with the levels in control cells (Fig. 5*B*). Indeed, multinucleated myotube formation was clearly reduced in Δ13Met siRNA-transfected cells on differentiation day 3 compared with that of control siRNA-transfected cells (Fig. 5*C*). The analysis of the extent of differentiation by measuring the total myotubular area disclosed a decreased differentiation in Δ13Met siRNA-transfected cells on days 3 and 4 (Fig. 5*D*). In addition, ~40% of MHC-positive cells from control siRNA-transfected cells contained more than two nuclei, whereas less than 30% of positive cells from Δ13Met siRNA-transfected cells contained more than two nuclei, confirming the decreased differentiation capacity of Δ13Met-depleted cells (Fig. 5*E*).

To evaluate whether Met depletion rescues the decreased differentiation of Δ13Met-depleted primary myoblast, cells were co-transfected with Δ13Met- and Met-specific siRNA followed by inducing differentiation. The reduced level of MHC-positive cells in Δ13Met-depleted cells was significantly overcome by depleting Met (Fig. 5*F*), suggesting that induction of

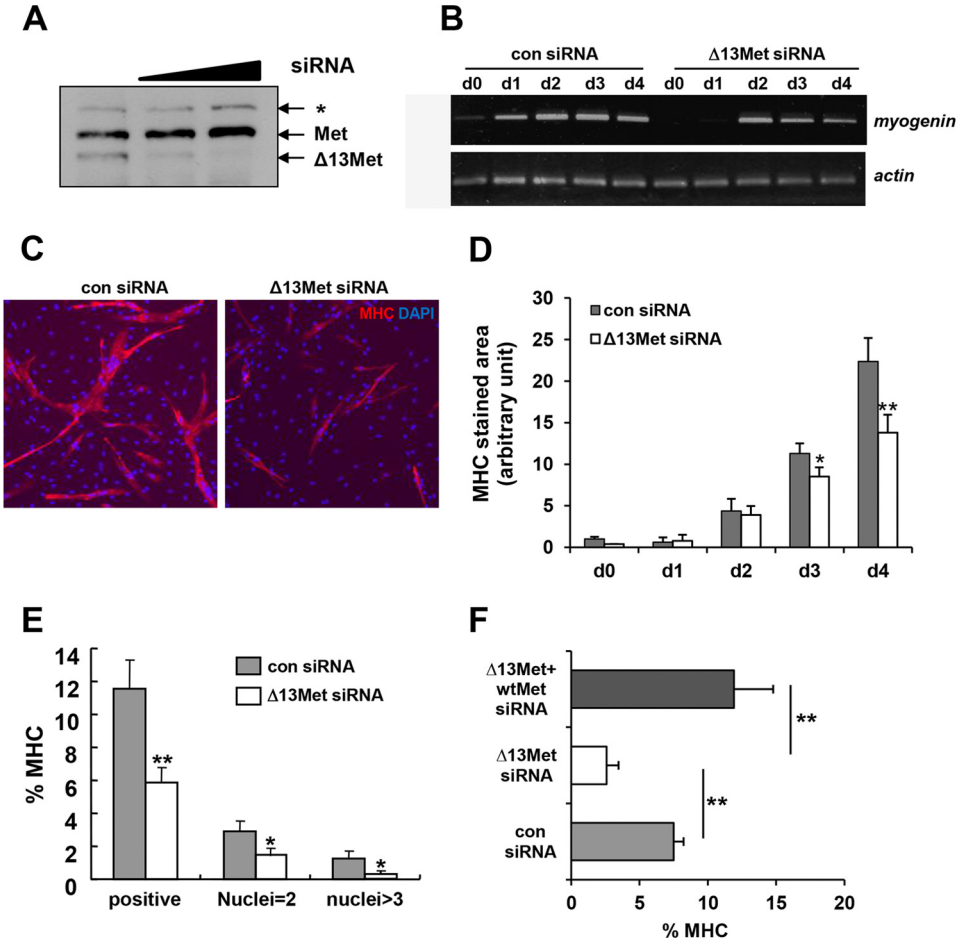

FIGURE 5. **Decrease in myoblast differentiation by Δ13Met-siRNA.** *A*, specific knockdown of Δ13Met with siRNA. NIH3T3 cells expressing both Met and Δ13Met were transfected with control siRNA or two different doses (50 or 100 nM) of Δ13Met-specific siRNA using Lipofectamine 2000. Control siRNA was used as for control transfection. Two days after transfection, cells were harvested and subjected to Western blotting. *B*, reduced level of myogenin mRNA induction by Δ13Met-specific siRNA transfection. Primary myoblasts were transfected with the indicated siRNA 1 day prior to differentiation, and the cells were harvested at the indicated times. RT-PCR analysis for myogenin was performed. Actin was used as the loading control. All samples were analyzed in triplicate, and the data are presented as means ± S.D. *C*, representative MHC staining of differentiated myoblasts. One day before differentiation, primary myoblasts cultured on coverslips were transfected with the indicated siRNA (100 nM). After induction of differentiation, coverslips were subjected to immunostaining for MHC expression. Representative images on differentiation day 3 are shown. DAPI was used to stain nuclei. *D*, the extent of differentiation is represented by arbitrary units of MHC-stained area, measured by Carl Zeiss AxioVision 4. *, $p < 0.05$; **, $p < 0.01$ compared with control siRNA at the corresponding day. *E*, decrease in myotube formation by Δ13Met-siRNA transfection. Myotubes showing MHC immunoreactivity with multinuclei were counted at day 3 in samples processed as for *C*. Myotubes with binuclei and multinuclei ($n \geq 3$) are separately counted. *, $p < 0.05$; **, $p < 0.01$ compared with con siRNA. *F*, primary myoblasts were co-transfected with Δ13Met and Met siRNAs followed by inducing differentiation for 3 days. The cells were immunostained for MHC as described in *C*. MHC-positive cells were counted in samples, and the extent of differentiation is quantified and represented as percentages of MHC-positive cells among total cells. *con*, control; *d*, day.

Δ13Met expression plays a role in the skeletal muscle differentiation process by inhibiting HGF/MET signaling.

Overexpression of Δ13Met Enhances Differentiation in Primary Human Skeletal Muscle Cells—To confirm the role of Δ13Met during muscle differentiation, we overexpressed Δ13Met in primary myoblasts followed by inducing differentiation. Primary myoblasts were transduced with Δ13Met-producing lentivirus or hrGFP-producing lentivirus, which was used as a control. Fig. 6*A* shows that the protein expression of Δ13Met was increased in a dose-dependent manner in the infected cells.

When the differentiation was induced in both cultures, the number of MHC-positive cells began to be seen at differentiation day 1, and the myotube formation was evident from day 2 in both cultures (Fig. 6*B*). However, the myotubes in Δ13Met-overexpressed myoblasts were longer and thinner than those in control cells, and the number of MHC-positive cells was significantly higher than that of control cells on differentiation days 2 and 3 (Fig. 6*C*). When the myotubes of day 3 were classified by the number of nuclei within each myotube, the myotubes in Δ13Met-overexpressed cells contained more nuclei than those in control (Fig. 6*D*). Specifically, over 50% of myotubes in Δ13Met-overexpressed cells had six or more nuclei in a single myotube, whereas only ~10% of myotubes in control cells had six or more nuclei. Furthermore, the mRNA of myogenin was induced 1 day earlier in Δ13Met-overexpressed cells than control cells (Fig. 6*E*). Because we used different batches of primary cells for the experiments shown in Figs. 4–6, variations in the day of myogenin induction or Δ13Met expression between different experiments were unavoidable. However, comparison between experimental groups in the same experimental setting was still possible because the same batch of primary cells was used for the specific experiment.

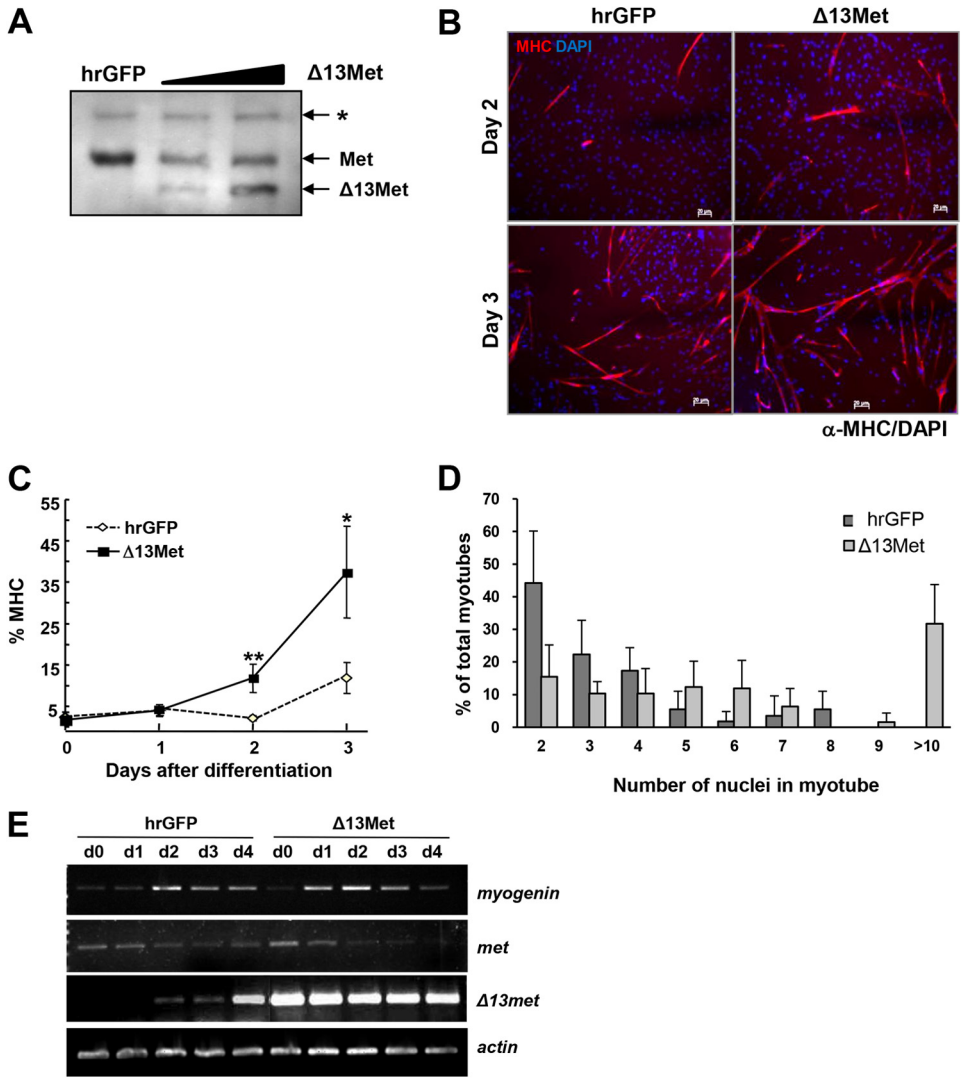

FIGURE 6. **Enhancement of myogenic differentiation by Δ13Met.** *A*, Δ13Met overexpression by lentivirus infection. Human primary myoblasts were infected with two different doses of Δ13Met-expressing or control hrGFP-expressing lentivirus prepared as described under "Experimental Procedures." Two days after infection, cells were subjected to Western blotting. *, Met precursor. *B*, representative MHC staining of differentiated myoblasts. One day before differentiation, myoblasts cultured on coverslips were infected with the corresponding lentiviruses. After differentiation, coverslips were subjected to immunostaining for MHC expression. Representative images of cells harvested on day 2 or 3 after differentiation are shown. *C*, increased MHC positivity of Δ13Met-expressing primary myoblasts. MHC-positive cells were counted in three different fields of each coverslip processed as for *B*. The extent of differentiation was represented as the percentage of MHC-positive cells among total cells. Samples were analyzed in triplicate. The data are presented as means ± S.D. *, $p < 0.05$; **, $p < 0.01$ compared with hrGFP-expressing cells. *D*, increase in myotube formation by Δ13Met expression. Multinucleated myotubes showing MHC positivity were counted and classified according to the number of nuclei which they possessed. Samples were analyzed in triplicate. The data are presented as means ± S.D. *E*, early induction of myogenin mRNA by Δ13Met. RT-PCR analysis for myogenin was performed, and actin was used as the loading control.

Collectively, these results strongly suggest that the induction of Δ13Met by alternative splicing significantly affects human skeletal muscle differentiation.

Δ13Met Accelerates Muscle Regeneration in Vivo—To address whether Δ13Met is a positive regulator of muscle regeneration *in vivo*, we injected Δ13Met-producing lentivirus into notexin-injured mouse TA muscle. We used a lentiviral vector encoding the murine version of Δ13Met instead of the human form in this experiment because human Met poorly binds murine HGF, whereas murine Met binds both human and murine HGF (39). Additionally, Δ13Met is hardly detected in mouse cells or tissues (our unpublished observation), so a knockdown approach was not an option to prove our hypothesis.

The inhibitory effects of the murine Δ13Met on HGF/Met signaling were confirmed because the increase of ERK1/2 and AKT phosphorylation by HGF exposure was inhibited by the presence of murine Δ13Met (Fig. 7*A*). Fluorescence from the hrGFP-expressing lentiviral vector control was observed as early as 1 day after the viral injection into TA muscle (Fig. 7*B*). Next, we evaluated the expression of endogenous Met in TA muscle by immunostaining transverse sections with anti-murine Met antibody (Fig. 7*C*). Positive immunoreactivities were detected near the nuclei localized outside muscle bundles, which are regarded as muscle satellite cells (*arrows*). In notexin-injured TA muscle, the cross-sectional area of muscle bundle was reduced, and bundles were dissociated from other bundles. However, the positive immunoreactivity of Met was increased, further suggesting that muscle precursor cells are activated as early as 1 day after notexin exposure by increasing the myogenic cell numbers.

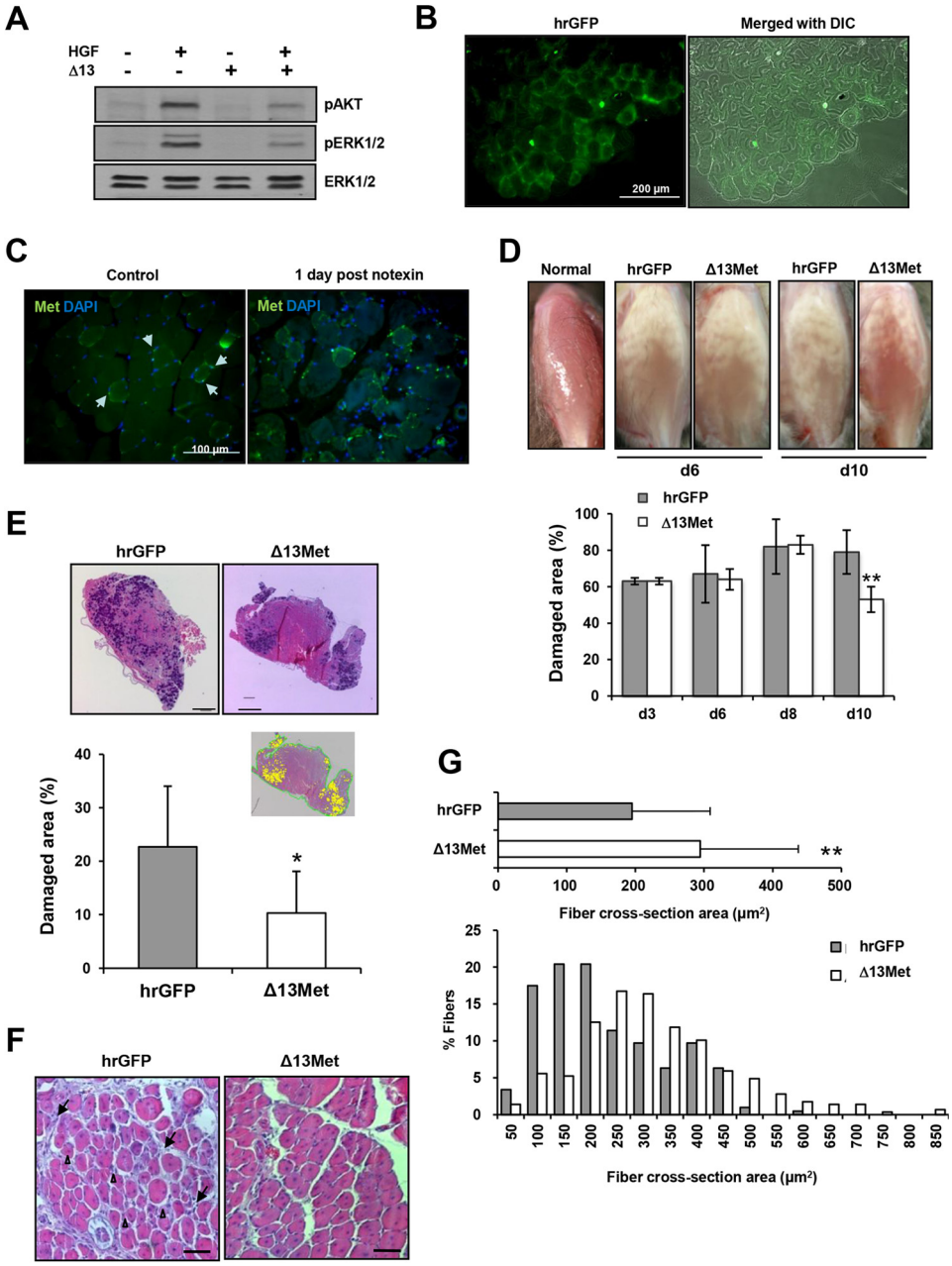

FIGURE 7. **Enhancement of muscle regeneration by Δ13Met overexpression.** *A*, NIH3T3 cells expressing murine Met were subsequently transfected with empty vector or murine version of Δ13Met. After serum depletion for 24 h, cells were treated with 20 units/ml of HGF for 10 min. Lysates from the samples were prepared and analyzed for ERK1/2 and AKT phosphorylation directly by Western blotting. *B*, representative fluorescence photomicrographs of hrGFP in cross-sections of TA muscle 1 day postintramuscular injection of hrGFP-expressing lentivirus. The muscles were surgically excised at the indicated day after injection, frozen, and sectioned transversely (8 μm) through the mid-belly region on a cryostat microtome at −20 °C. *C*, the cross-sections of TA muscle were immunostained with anti-murine Met antibody (*green*). DAPI was used to stain nuclei (*blue*). *D*, comparison of the surface of TA muscle between hrGFP and Δ13Met-injected mice. Representative photomicrographs were taken at the indicated day postinjury (*left panel*). The estimated damaged area (*white-colored area*) was measured by AxioVision version 4 (*right panel*). The *p* values were determined using two-way analysis of variance. **, $p < 0.01$ compared with hrGFP-injected TA muscle. *E*, effect of Δ13Met expression in TA muscle regeneration. Cross-sections of hrGFP or Δ13Met-injected TA muscle, which was harvested at day 10 postinjury, were stained with hematoxylin/eosin (*left panel*). *Scale bar*, 200 μm. The damaged myofibers stained *dark purple* were depicted as *yellow dots* using Image-Pro Plus 4.5 after photographed by digital camera (*right panel*, *inset*). The obtained results were quantified and represented in a form of a bar graph (*right panel*). *, $p < 0.05$ compared with hrGFP-injected muscle. *F*, representative photomicrographs of hematoxylin/eosin-stained transverse TA muscle section. Note the greater number of infiltrated lymphocytes between and on the muscle fibers (*arrows*) and the small, irregular shape of damaged muscle fibers in hrGFP-injected muscle (*arrowheads*). *Scale bar*, 20 μm. *G*, comparison of the cross-sectional area of myofibers between hrGFP and Δ13Met-injected muscle (*upper panel*). The distribution of the cross-sectional area of myofibers measured by AxioVision version 4 was plotted (*lower panel*). The data are means ± S.D. *, $p < 0.05$; **, $p < 0.01$ compared with hrGFP-injected muscle. *d*, day; *DIC*, differential interference contrast.

The surface of TA muscle turned to be rather white and edematous on the third day after the notexin injection, and the damaged area was expanded up to 80% until day 8 in both groups (Fig. 7*D*, *left panel*). The white-colored damaged surface areas remained as 80% on day 10 after injury in control mice, whereas the color of the surface was significantly recovered in the Δ13Met-injected mice, and the damaged surface area, measured by image analysis, was significantly diminished at day

10 (Fig. 7*D*, *right panel*; $p < 0.01$ compared with control). In support of the above observations, hematoxylin/eosin staining of transverse sections of TA muscles clearly revealed reduction of the damaged fibers stained *dark purple* in Δ13Met-introduced TA muscle compared with controls (Fig. 7*E*, *left panels*). The damaged fibers were depicted as *yellow dots* that were quantified using Image-Pro Plus 4.5 (Fig. 7*E*, *right panel*, *inset*). The mean damaged area of Δ13Met-injected mice was reduced by ~60% compared with the controls (Fig. 7*E*, *right panel*; $p < 0.05$). Moreover, the clearance of inflammation and the replacement of damaged myofibers by newly formed fibers, evidenced by the central localization of nuclei, were more clearly observed in the Δ13Met-introduced TA muscle compared with the control mice (Fig. 7*F*). In addition, the median cross-sectional area of myofibers was significantly increased in the Δ13Met-introduced group compared with the control group (Fig. 7*G*, *upper panel*; $n = 300$, $p < 0.05$). A plot of the area of each myofiber as a function of frequency distributions showed a rightward shift in the Δ13Met-introduced muscle, indicating an evident increase in the percentage of larger fibers (Fig. 7*G*, *lower panel*).

Collectively, these data clearly show that ectopic expression of Δ13Met enhances muscle regeneration *in vivo*. Although Δ13Met is not expressed in murine skeletal muscle tissue, the above *in vivo* effect of expression of artificial murine Δ13Met on muscle regeneration shows the regulatory effects of Δ13Met in skeletal muscle differentiation and/or regeneration, as well as a possibility that the human form of Δ13Met also enhances muscle regeneration in human skeletal muscle tissues.

DISCUSSION

Regarding muscle differentiation and/or regeneration, HGF is responsible for stimulation of satellite cell activation after muscle injury (15) and migration of muscle precursors into the limb buds of developing embryos (11, 40). Although HGF was first shown to induce DNA synthesis in quiescent satellite cells, thereby driving them into the cell cycle, it also inhibits myogenesis in cultured myoblasts (18). When HGF was ectopically expressed in primary satellite cells, it suppressed the activation of muscle regulatory gene reporter constructs (MCK, MRF4, MEF2, and 4Rtk-CAT), as well as the gene expression of MyoD, myogenin, and MHC (22). These data imply that the effect of HGF on muscle regeneration probably depends on whether HGF is applied before or after the activation of satellite cells. Because HGF is normally present in the extracellular matrix surrounding muscle fibers and the activated satellite cells, a regulatory system to inhibit HGF/Met signaling at the right time is required to achieve successful myotube formation during muscle regeneration. It has been reported that the transcription of *hgf* and c-*met* genes is down-regulated when myoblasts stop proliferating and begin to differentiate, providing a down-regulation mechanism of HGF/Met signaling (15).

Important results of this study indicate that a novel Met variant is expressed in human skeletal muscle that is produced by alternative splicing. Exon 13 skipping in the mRNA induces a reading frameshift followed by an early termination, which produces C-terminally truncated Met (Δ13Met). The structure is very similar to previously reported Met recombinants, which had the extracellular domain of Met and showed HGF/Met signaling inhibition by interfering with HGF binding to Met and Met homodimerization (34, 40). Met-934, one of the splicing variants of Met, is composed of the first 12 exons of c-*met* followed by an extension of the twelfth exon and a stop codon, implying a Met variant resembling Δ13Met (41). The authors obtained this variant by clustering and assembling the information from dbEST (GenBank™) and the human genome. Similar to Δ13Met, this form reduces Met activation-induced cell proliferation and survival. However, the authors used an artificial fusion protein with the Fc portion of human IgG1 instead of the endogenous form for the functional study. In addition, the endogenous expression of this truncated isoform was not documented. Interestingly, our data prove that both mRNA and protein of Δ13Met are expressed in human skeletal muscle, and the protein is localized in the plasma membrane, which could be released by proteolytic cleavage. Moreover, the inhibitory effect of Δ13Met in HGF/Met signaling pathways corresponds with results from other inhibitory Met recombinants in which Δ13Met overexpression inhibits HGF-induced Met phosphorylation, ERK1/2 signaling, cell proliferation, and cell migration. Our data suggest that Δ13Met expression caused by alternative splicing is a novel mechanism of down-regulating HGF/Met signaling.

Several elements are involved in the regulation of alternative splicing. One of these elements is direct or indirect interactions of *cis*-acting regulatory elements and *trans*-acting activators or repressors of splicing (41). Ron, another member of the scatter factor receptor family like Met, has an alternatively spliced isoform (ΔRon) generated by the deletion of exon 11 (42). It has been reported that the deletion of exon 11 of Ron is controlled by an exonic splicing silencer and exonic splicing enhancer located in exon 12 and that SF2/ASF, a *trans*-acting serine- and arginine-rich splicing factor (SR proteins), binds directly to exonic splicing enhancer and enhances its splicing activity (43). We found several *cis*-acting elements around exons 12–14 of c-*met* using ESE Finder program. In addition, SR proteins displayed different expression patterns between proliferating and differentiating primary human skeletal muscle cells.[6] The possibility of the involvement of specific *cis*-acting elements and SR proteins in the regulation of Δ13Met expression is presently under investigation.

The cellular localization of Δ13Met is predicted to be extracellular including cell wall by PSORT, a computer program for the prediction of protein localization sites in cells. However, the presence of Δ13Met was not identified in the conditioned medium, but rather a shedding Met released from Δ13Met was identified, suggesting that Δ13Met is localized on the plasma membrane where ectodomain shedding is occurred by metalloproteases (34). Our results of immunostaining and cellular fractionation also support the presence of Δ13Met on the plasma membrane, suggesting possible dimerization between Met and Δ13Met. Although we have addressed whether Δ13Met forms a heterodimer with wild type Met by using cross-linking agents but failed to confirm its presence (data not

[6] M. Park, unpublished observations.

shown), we suspect that the structural conformation of Δ13Met on the plasma membrane might not be the same as that of Met that spans through the plasma membrane and that might make unfavorable conditions for heterodimerization.

The most important finding in the study is a novel mechanism for down-regulating HGF/Met signaling during muscle cell differentiation. We prove that Δ13Met expression is up-regulated during muscle differentiation (Fig. 4), and the abrogation of Δ13Met expression with a specific siRNA results in a decrease of muscle differentiation (Fig. 5). Furthermore, ectopic expression of Δ13Met significantly enhances muscle differentiation both *in vitro* and *in vivo* (Figs. 6 and 7). These data led us to our view that after the activation and proliferation of myoblasts in early phase of skeletal muscle regeneration and/or differentiation, increase of Δ13Met expression relative to Met contributes to the down-regulation of HGF/Met signaling, which subsequently leads to the stimulation of terminal muscle cell differentiation.

To the best of our knowledge, this is the first report on the role of an alternatively spliced form of Met in human physiology. Furthermore, the activating role of Δ13Met in skeletal muscle differentiation through its antagonistic activity against HGF may be valuable in the development of new strategies for enhancing muscle differentiation/regeneration in clinical situations.

Acknowledgments—We thank Dr. Vande Woude for Met cDNA, Dr. Kim for human EF1$_\alpha$ gene promoter, Dr. Hope for WPRE, and Minguk Cho for the artwork.

REFERENCES

1. Schultz, E., and McCormick, K. M. (1994) Skeletal muscle satellite cells. *Rev. Physiol. Biochem. Pharmacol.* **123,** 213–257
2. Relaix, F., and Zammit, P. S. (2012) Satellite cells are essential for skeletal muscle regeneration: the cell on the edge returns centre stage. *Development* **139,** 2845–2856
3. Hawke, T. J., and Garry, D. J. (2001) Myogenic satellite cells: physiology to molecular biology. *J. Appl. Physiol.* **91,** 534–551
4. Florini, J. R., Ewton, D. Z., and Roof, S. L. (1991) Insulin-like growth factor-I stimulates terminal myogenic differentiation by induction of myogenin gene expression. *Mol. Endocrinol.* **5,** 718–724
5. Austin, L., and Burgess, A. W. (1991) Stimulation of myoblast proliferation in culture by leukaemia inhibitory factor and other cytokines. *J. Neurol. Sci.* **101,** 193–197
6. Fiaschi, T., Magherini, F., Gamberi, T., Modesti, P. A., and Modesti, A. (2014) Adiponectin as a tissue regenerating hormone: more than a metabolic function. *Cell. Mol. Life Sci.* **71,** 1917–1925
7. Trusolino, L., Bertotti, A., and Comoglio, P. M. (2010) MET signalling: principles and functions in development, organ regeneration and cancer. *Nat. Rev. Mol. Cell Biol.* **11,** 834–848
8. Liu, Y. (2002) Hepatocyte growth factor and the kidney. *Curr. Opin. Nephrol. Hypertens.* **11,** 23–30
9. Christ, B., and Brand-Saberi, B. (2002) Limb muscle development. *Int. J. Dev. Biol.* **46,** 905–914
10. Cross, J. C., Baczyk, D., Dobric, N., Hemberger, M., Hughes, M., Simmons, D. G., Yamamoto, H., and Kingdom, J. C. (2003) Genes, development and evolution of the placenta. *Placenta* **24,** 123–130
11. Yamane, A., Amano, O., and Slavkin, H. C. (2003) Insulin-like growth factors, hepatocyte growth factor and transforming growth factor-α in mouse tongue myogenesis. *Dev. Growth Differ.* **45,** 1–6
12. Karalaki, M., Fili, S., Philippou, A., and Koutsilieris, M. (2009) Muscle regeneration: cellular and molecular events. *In Vivo* **23,** 779–796
13. Cornelison, D. D., and Wold, B. J. (1997) Single-cell analysis of regulatory gene expression in quiescent and activated mouse skeletal muscle satellite cells. *Dev. Biol.* **191,** 270–283
14. Allen, R. E., and Rankin, L. L. (1990) Regulation of satellite cells during skeletal muscle growth and development. *Proc. Soc. Exp. Biol. Med.* **194,** 81–86
15. Tatsumi, R., Anderson, J. E., Nevoret, C. J., Halevy, O., and Allen, R. E. (1998) HGF/SF is present in normal adult skeletal muscle and is capable of activating satellite cells. *Dev. Biol.* **194,** 114–128
16. Tatsumi, R., Hattori, A., Ikeuchi, Y., Anderson, J. E., and Allen, R. E. (2002) Release of hepatocyte growth factor from mechanically stretched skeletal muscle satellite cells and role of pH and nitric oxide. *Mol. Biol. Cell* **13,** 2909–2918
17. Webster, M. T., and Fan, C. M. (2013) c-MET regulates myoblast motility and myocyte fusion during adult skeletal muscle regeneration. *PLoS One* **8,** e81757
18. Anastasi, S., Giordano, S., Sthandier, O., Gambarotta, G., Maione, R., Comoglio, P., and Amati, P. (1997) A natural hepatocyte growth factor/scatter factor autocrine loop in myoblast cells and the effect of the constitutive Met kinase activation on myogenic differentiation. *J. Cell Biol.* **137,** 1057–1068
19. Miller, K. J., Thaloor, D., Matteson, S., and Pavlath, G. K. (2000) Hepatocyte growth factor affects satellite cell activation and differentiation in regenerating skeletal muscle. *Am. J. Physiol. Cell Physiol.* **278,** C174–C181
20. Jennische, E., Ekberg, S., and Matejka, G. L. (1993) Expression of hepatocyte growth factor in growing and regenerating rat skeletal muscle. *Am. J. Physiol.* **265,** C122–C128
21. Flann, K. L., Rathbone, C. R., Cole, L. C., Liu, X., Allen, R. E., and Rhoads, R. P. (2014) Hypoxia simultaneously alters satellite cell-mediated angiogenesis and hepatocyte growth factor expression. *J. Cell. Physiol.* **229,** 572–579
22. Gal-Levi, R., Leshem, Y., Aoki, S., Nakamura, T., and Halevy, O. (1998) Hepatocyte growth factor plays a dual role in regulating skeletal muscle satellite cell proliferation and differentiation. *Biochim. Biophys. Acta* **1402,** 39–51
23. Liu, Y. (1998) The human hepatocyte growth factor receptor gene: complete structural organization and promoter characterization. *Gene* **215,** 159–169
24. Kim, D. W., Uetsuki, T., Kaziro, Y., Yamaguchi, N., and Sugano, S. (1990) Use of the human elongation factor 1α promoter as a versatile and efficient expression system. *Gene* **91,** 217–223
25. Zufferey, R., Donello, J. E., Trono, D., and Hope, T. J. (1999) Woodchuck hepatitis virus posttranscriptional regulatory element enhances expression of transgenes delivered by retroviral vectors. *J. Virol.* **73,** 2886–2892
26. Reiser, J. (2000) Production and concentration of pseudotyped HIV-1-based gene transfer vectors. *Gene Ther.* **7,** 910–913
27. Foulstone, E. J., Huser, C., Crown, A. L., Holly, J. M., and Stewart, C. E. (2004) Differential signalling mechanisms predisposing primary human skeletal muscle cells to altered proliferation and differentiation: roles of IGF-I and TNFα. *Exp. Cell Res.* **294,** 223–235
28. Schertzer, J. D., and Lynch, G. S. (2006) Comparative evaluation of IGF-I gene transfer and IGF-I protein administration for enhancing skeletal muscle regeneration after injury. *Gene Ther.* **13,** 1657–1664
29. Shinomiya, N., Gao, C. F., Xie, Q., Gustafson, M., Waters, D. J., Zhang, Y.-W., and Vande Woude, G. F. (2004) RNA interference reveals that ligand-independent met activity is required for tumor cell signaling and survival. *Cancer Res.* **64,** 7962–7970
30. Lee, C. C., and Yamada, K. M. (1994) Identification of a novel type of alternative splicing of a tyrosine kinase receptor. Juxtamembrane deletion of the c-met protein kinase C serine phosphorylation regulatory site. *J. Biol. Chem.* **269,** 19457–19461
31. Lee, J. H., Gao, C. F., Lee, C. C., Kim, M. D., and Vande Woude, G. F. (2006) An alternatively spliced form of Met receptor is tumorigenic. *Exp. Mol. Med* **38,** 565–573
32. Lin, J. C., Naujokas, M., Zhu, H., Nolet, S., and Park, M. (1998) Intron-exon structure of the MET gene and cloning of an alternatively-spliced Met isoform reveals frequent exon-skipping of a single large internal exon. *Oncogene* **16,** 833–842

33. Rodrigues, G. A., Naujokas, M. A., and Park, M. (1991) Alternative splicing generates isoforms of the met receptor tyrosine kinase which undergo differential processing. *Mol. Cell. Biol.* **11,** 2962–2970
34. Arribas, J., and Borroto, A. (2002) Protein ectodomain shedding. *Chem. Rev.* **102,** 4627–4638
35. Kong-Beltran, M., Stamos, J., and Wickramasinghe, D. (2004) The Sema domain of Met is necessary for receptor dimerization and activation. *Cancer Cell* **6,** 75–84
36. Ponzetto, C., Bardelli, A., Zhen, Z., Maina, F., dalla Zonca, P., Giordano, S., Graziani, A., Panayotou, G., and Comoglio, P. M. (1994) A multifunctional docking site mediates signaling and transformation by the hepatocyte growth factor/scatter factor receptor family. *Cell* **77,** 261–271
37. Seger, R., and Krebs, E. G. (1995) The MAPK signaling cascade. *FASEB J.* **9,** 726–735
38. Chernyavsky, A. I., Arredondo, J., Karlsson, E., Wessler, I., and Grando, S. A. (2005) The Ras/Raf-1/MEK1/ERK signaling pathway coupled to integrin expression mediates cholinergic regulation of keratinocyte directional migration. *J. Biol. Chem.* **280,** 39220–39228
39. Bhargava, M., Joseph, A., Knesel, J., Halaban, R., Li, Y., Pang, S., Goldberg, I., Setter, E., Donovan, M. A., and Zarnegar, R. (1992) Scatter factor and hepatocyte growth factor: activities, properties, and mechanism. *Cell Growth Differ.* **3,** 11–20
40. Bladt, F., Riethmacher, D., Isenmann, S., Aguzzi, A., and Birchmeier, C. (1995) Essential role for the c-met receptor in the migration of myogenic precursor cells into the limb bud. *Nature* **376,** 768–771
41. Garcia-Blanco, M. A., Baraniak, A. P., and Lasda, E. L. (2004) Alternative splicing in disease and therapy. *Nat. Biotechnol.* **22,** 535–546
42. Collesi, C., Santoro, M. M., Gaudino, G., and Comoglio, P. M. (1996) A splicing variant of the RON transcript induces constitutive tyrosine kinase activity and an invasive phenotype. *Mol. Cell. Biol.* **16,** 5518–5526
43. Ghigna, C., Giordano, S., Shen, H., Benvenuto, F., Castiglioni, F., Comoglio, P. M., Green, M. R., Riva, S., and Biamonti, G. (2005) Cell motility is controlled by SF2/ASF through alternative splicing of the Ron protooncogene. *Mol. Cell* **20,** 881–890
44. Jeffers, M., Schmidt, L., Nakaigawa, N., Webb, C. P., Weirich, G., Kishida, T., Zbar, B., and Vande Woude, G. F. (1997) Activating mutations for the Met tyrosine kinase receptor in human cancer. *Proc. Natl. Acad. Sci. U.S.A.* **94,** 11445–11450
45. Lee, J. H., Han, S. U., Cho, H., Jennings, B., Gerrard, B., Dean, M., Schmidt, L., Zbar, B., and Vande Woude, G. F. (2000) A novel germ line juxtamembrane Met mutation in human gastric cancer. *Oncogene* **19,** 4947–4953